Tamaki, K., Suyehiro, K., Allan, J., McWilliams, M., et al., 1992
Proceedings of the Ocean Drilling Program, Scientific Results, Vol. 127/128, Pt. 2

79. DIAGENETIC REACTIONS IN DEEPLY BURIED SEDIMENTS OF THE JAPAN SEA: A SYNTHESIS OF INTERSTITIAL-WATER CHEMISTRY RESULTS FROM LEGS 127 AND 128[1]

Richard W. Murray,[2] Hans J. Brumsack,[3] Marta T. von Breymann,[4] Anne A. Sturz,[5] Robert B. Dunbar,[6] and Joris M. Gieskes[5]

ABSTRACT

Shipboard and shore-based analyses of ~230 interstitial-water samples gathered at six sites during ODP Legs 127 and 128 indicate that diagenetic reactions within sediment columns throughout the Japan Sea record the influence of bacterial degradation of organic matter, transformation of amorphous biogenic opaline silica to opal-CT, and formation and alteration of carbonate phases, as well as alteration of crystalline basement and volcanic ash.

Organic matter oxidation not only affects the distribution of oxidants (SO_4, Mn, and CO_2) and dissolved metabolites (alkalinity, NH_4, and PO_4), but also controls the distribution of many authigenic solid phases. Site 794, located deep in the Yamato Basin, is the only site where sulfate is not completely consumed, whereas Sites 798 and 799 record the total consumption of sulfate at shallow depths and concomitant extreme generation of alkalinity, NH_4, and PO_4. Authigenic carbonates, phosphates, and barite also record the importance of bacterial activity. The diagenetic opal-A/opal-CT transition is a notable chemical, diagenetic, and stratigraphic horizon that occurs more shallowly in the basinal sites because of their greater geothermal gradient. Due to its effect on the porosity and permeability of the involved lithologies, the siliceous phase transformation effectively restricts diffusion between reactions occurring in the uppermost sediment column from those involved in deep basement alteration. Processes that influence dissolved Ca, Mg, Sr, and alkalinity tend to be preferentially dominant at either basinal (Site 794, 795, and 797) or ridge (all other) sites, due to the distinctly different depths and sedimentation rates of the two depositional regimes. At basinal sites, where sediment accumulation is relatively slow and occurs below the CCD, basement alteration is the dominant influence on dissolved Ca and Mg profiles. At ridge sites, where accumulation is relatively fast and occurs above the CCD, diagenetic reactions such as calcite dissolution, inorganic carbonate precipitation, dolomitization, and siderite/ankerite formation control Ca and Mg behavior. Basement alteration reactions are responsible for large overall decreases in Mg, K, Rb, Li, B, $\delta^{18}O$, δD, $^{87}Sr/^{86}Sr$, and Na with depth, as well as for increases in Ca and Sr. Alteration of ash in the sediment column also influences these downhole profiles. Site 795, in the Japan Basin, preserves the greatest diagenetic signal of basement alteration. Gradients resulting from basement alteration document the importance of diffusive chemical exchange between the endogenic and exogenic reservoirs.

INTRODUCTION

The Japan Sea is one of the most thoroughly studied backarc basins in the western Pacific region. Since the initiation of extension and rifting in the late Oligocene–early Miocene, the complex tectonic interplay between the subduction of the Pacific plate and basinal extension has resulted in the generation of a variety of physiographic and depositional provinces in which sedimentation has recorded the geologic and paleoceanographic history of the Japan Sea and its margins. These provinces include (1) deep basins, such as the Japan and Yamato basins; (2) block-faulted ridges, such as the Yamato Rise; and (3) north-trending tectonic ridges and basins associated with active thrust and reverse faults along the eastern margin of the Japan Sea (Tamaki, Pisciotto, Allan, et al., 1990). Ocean Drilling Program (ODP) Legs 127 and 128 collectively studied in detail each of these depositional provinces. Comparing interstitial-water profiles of the suite of chemical constituents analyzed from each province allows assessment of many different diagenetic processes acting within the varying lithologic, paleoceanographic, and geologic regimes.

The ambitious cruise and post-cruise interstitial-water analytical programs of Legs 127 and 128 resulted in thorough elemental and isotopic analysis of a total of ~230 samples from six cored sites throughout the Japan Sea (Fig. 1). Many sedimentary horizons were sampled in replicate, due to the combined use on both legs of the standard ODP stainless-steel Manheim squeezer (Manheim and Sayles, 1974) and the new Teflon-lined squeezer used for extruding noncontaminated interstitial waters (Brumsack et al., this volume). The shipboard and shore-based data sets and analytical techniques are tabulated and described elsewhere (Tamaki, Pisciotto, Allan, et al., 1990; Ingle, Suyehiro, von Breymann, et al., 1990; Brumsack et al., this volume; Sturz et al., this volume).

Interstitial waters in the Japan Sea record the effects of fluid/solid exchange reactions associated with the bacterial degradation of organic matter, alteration of volcanic ash, carbonate mineral formation and alteration, diagenetic dissolution and reprecipitation of biogenic SiO_2, and basement alteration affiliated with clay mineral crystallization. In association with the differences in depositional style among the three physiographic provinces listed previously, one of these processes usually dominates over the others through a particular stratigraphic zone. Interstitial-water profiles from Site 796 (Okushiri Ridge), in addition to recording fluid/solid reaction, also display an influence from gas hydrates (Tamaki, Pisciotto, Allan, et al., 1990), which serves to complicate the detailed interpretation of the other diagenetic mechanisms. This paper synthesizes the results of the shipboard and shore-based interstitial-water programs of Legs 127 and 128 and attempts to resolve the relative contributions of each of the fluid/solid exchange mechanisms throughout the Japan Sea. We discuss these contributions in relative stratigraphic order (i.e., organic degradation first, basement alteration processes last), although this does not imply any relative dominance or importance of process.

---

[1] Tamaki, K., Suyehiro, K., Allan, J., McWilliams, M., et al., 1992. *Proc. ODP, Sci. Results,* 127/128, Pt. 2: College Station, TX (Ocean Drilling Program).

[2] Department of Geology and Geophysics, University of California at Berkeley, Berkeley, CA 94720, U.S.A. (Present address: Graduate School of Oceanography, University of Rhode Island, Narragansett, RI 02882, U.S.A.).

[3] Geochemisches Institut, Goldschmidtstr. 1, D-3400, Göttingen, Federal Republic of Germany.

[4] Ocean Drilling Program, Texas A&M University, 1000 Discovery Drive, College Station, TX 77845, U.S.A. (Present address: GEOMAR, Wischhofstrasse 1-3, Gebaude 12, D-2300 Kiel 14, Federal Republic of Germany).

[5] Scripps Institution of Oceanography, University of California, San Diego, CA 92093, U.S.A. (Sturz, present address: Department of Marine and Environmental Studies, University of San Diego, Alcala Park, San Diego, CA 92110, U.S.A.).

[6] Department of Geology and Geophysics, Rice University, P.O. Box 1892, Houston, TX 77251, U.S.A.

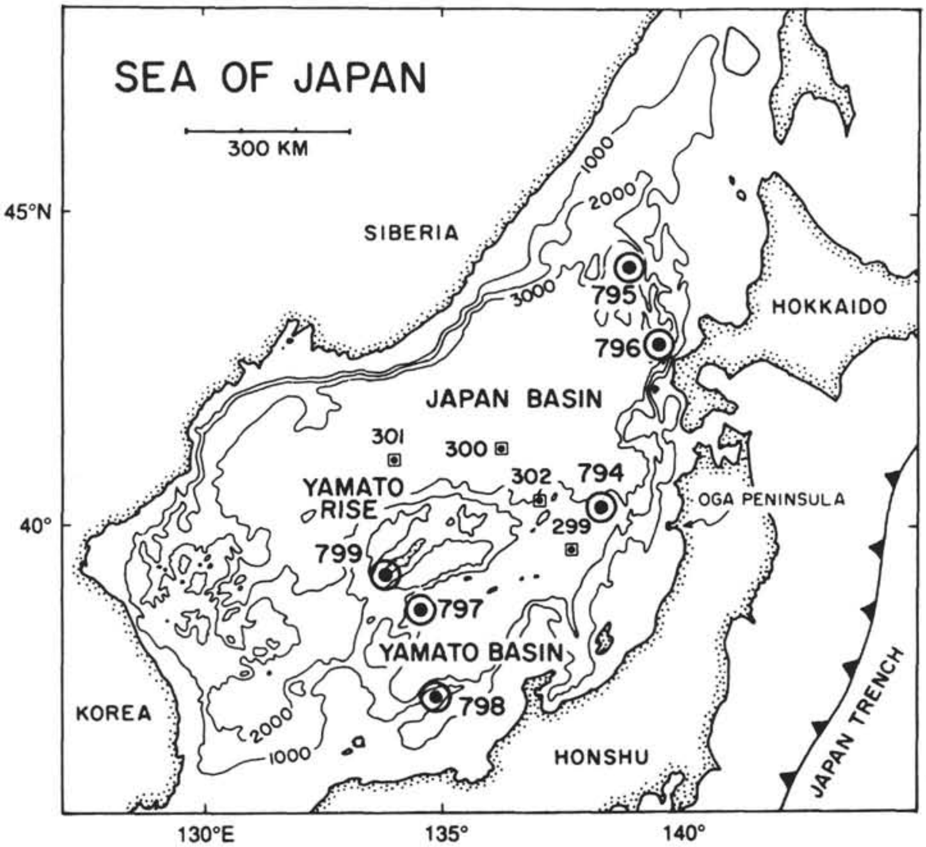

Figure 1. Map of the Japan Sea showing the location of sites drilled by ODP Legs 127 and 128, with bathymetry in meters. Deep Sea Drilling Project Sites 299–302 are shown as well. Modified from Ingle, Suyehiro, von Breymann, et al. (1990).

ORGANIC MATTER DIAGENESIS

All sites drilled in the Japan Sea are characterized by the decomposition of organic carbon, most commonly by sulfate reduction. Other terminal electron acceptors, however, are also involved in the bacterial degradation of organic carbon, although to a lesser degree. High sampling resolution in the upper sections of Hole 798B permits detailed examination of the mechanisms of organic matter degradation during early diagenesis, where the decrease in Mn concentrations through the upper 5 m, closely followed by sulfate utilization (Fig. 2), clearly illustrates the sequential pathways of bacterially mediated organic carbon oxidation (Froelich et al., 1979). Also, decomposition of organic carbon below the sulfate reduction zone proceeds by carbonate reduction and methanogenesis (Fig. 2). Furthermore, Hole 798B is particularly interesting because, although bacterial populations and activities in the sediment decreased with depth, significant microbial populations were documented as existing even in the deepest samples (518 m below seafloor (mbsf); Cragg et al., this volume). Bacterial activity measurements show sulfate reduction to be quantitatively more important than methanogenesis, which peaks beneath the maximum in sulfate reduction (Cragg et al., this volume).

Sulfate is utilized at all sites (Fig. 3), with the consequent release of the organic metabolites total dissolved CO_2, ammonium, and phosphate. The relationship between interstitial-water sulfate gradient and sedimentation rate (Fig. 4; Berner, 1980) results from the interaction of sulfate diffusion, bacterial sulfate-reduction, and sediment accumulation. This relationship has been further studied utilizing the sulfur isotopic signature of the dissolved sulfate (Brumsack et al., this volume). In the slowly accumulating sediments at Site 794, diffusion from overlying seawater precludes the exhaustion of the ^{32}S reservoir. This is in direct contrast with the high $\delta^{34}S$ values (+93 ‰ CDT) measured at Site 797, where the lack of communication with the overlying seawater and the preferential utilization of the lighter isotope by bacteria during organic carbon oxidation results in depletion of the light ^{32}S nuclide.

Dissolved ammonium and phosphate are metabolic products of the decomposition of organic carbon, and, therefore, their respective concentrations increase in the upper sediment sections (Fig. 3). Because phosphate is preferentially released during organic matter degradation, the phosphate maximum usually occurs at a shallower depth than the ammonium maximum (Balzer, 1984), as shown in Figure 3. The phosphate decrease in the deeper sections of all sites suggests a diagenetic uptake of dissolved phosphate into sedimentary mineral phases, as described in Japan Sea sediments by Föllmi and von Breymann (this volume). The decreasing ammonium concentrations most likely record ion-exchange reactions on clay mineral surfaces (Rosenfeld, 1979), and subsequent incorporation into clay mineral interlayers (Wlotzka, 1972).

The alkalinity increase in the upper section of the holes (Fig. 3) reflects bicarbonate production during bacterial degradation of organic matter. This increase is followed by a decrease at depth that results from a combination of processes, including carbonate reduction and precipitation of authigenic carbonates. Carbonate diagenesis in the Japan Sea is discussed elsewhere in this paper, as well as by Matsumoto (this volume) and Sturz et al. (this volume). Dissolved CO_2 in the interstitial fluids of Site 799 records $\delta^{13}C = -24$ ‰ as shallow as 16 mbsf (Fig. 5; Sturz et al., this volume), indicating the oxidation of organic matter ($\delta^{13}C = -22$ ‰). Deeper sections at this site (>200 mbsf) record $\delta^{13}C$ of the fluids ranging from -5 ‰ to -10 ‰, reflecting a mixing among buried oceanic dissolved carbonate ($\delta^{13}C = +0.5$ ‰), meta-

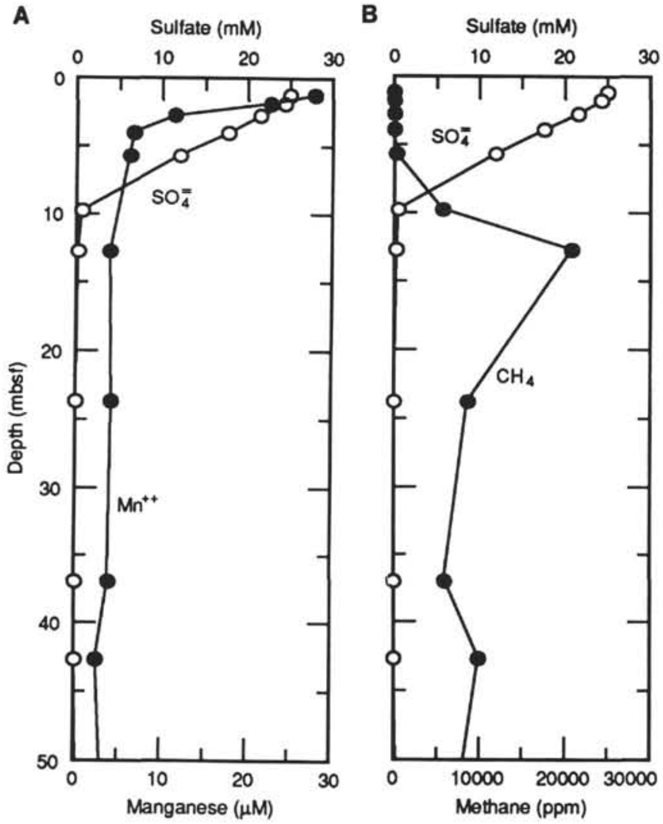

Figure 2. **A.** High-resolution distribution of dissolved Mn (closed symbols) and sulfate (open symbols) in the upper 50 mbsf of Hole 798B. Note earlier (i.e., shallower) utilization of Mn, as shown by its steeper gradient in the upper 10 mbsf. From Ingle, Suyehiro, von Breymann, et al. (1990). **B.** High-resolution distribution of dissolved sulfate (open symbols), indicating the onset of methanogenesis by the increase in methane concentration (closed symbols) after sulfate depletion in the upper 50 mbsf of Hole 798B. From Ingle, Suyehiro, von Breymann, et al. (1990).

bolic CO_2 generated from the mineralization of organic carbon ($\delta^{13}C = -22$ ‰), and dissolution/recrystallization of fossil carbonates ($\delta^{13}C = +2$ ‰; McCorkle, 1987; Emerson and Bender, 1981).

DIAGENESIS OF BIOGENIC SILICA

The dissolved silica concentration-depth profiles monitor the transition from amorphous biogenic opal to progressively more ordered diagenetic silica phases. These siliceous phase transitions are widespread and exert a strong control over other diagenetic reactions occurring in the Japan Sea. The increasing dissolution with depth of diatom tests constructed of metastable opal-A contributes dissolved silica to the interstitial waters sampled at all sites cored during Legs 127 and 128 (Fig. 6A). Although the amount of biogenic silica included in the sediment column varies between sites, with, for example, Site 798 having a relatively low siliceous component (Ingle, Suyehiro, von Breymann, et al., 1991), all profiles of dissolved silica are relatively similar down to ~300 mbsf (Fig. 6A).

At the deep basinal sites drilled during Leg 127, the concentration of dissolved silica in the interstitial waters increases steadily until ~290–325 mbsf (*in-situ* temperatures of ~36°–43°C), whereupon dissolved silica concentrations decrease sharply from values of ~1400 to 800 μM (Fig. 6A). This clearly defined decrease in dissolved silica marks the siliceous phase transition from opal-A to opal-CT. This transformation occurs at greater depths for the shallower sites drilled during Leg 128, where it is found from ~420 to ~450 mbsf (Fig. 6A) and at *in-situ* temperatures of ~38°–45°C, reflecting the lower geothermal gradients at Sites 798 and 799 (~100°–110°C/km; Ingle, Suyehiro, von Breymann, et al., 1990) relative to the gradient at the deep basinal sites (~120°–135°C/km; Tamaki, Pisciotto, Allan, et al., 1990). The time-temperature conditions of the occurrence of this transition in the Japan Sea agree well with previous estimates for the time and temperature necessary for the initiation of opal-CT formation (Fig. 6B; Hein et al., 1978). Diatoms are essentially absent from the subsequent opal-CT–bearing sediment, and the opal-A/opal-CT transformation usually defines a prominent lithologic change from diatom ooze and silty claystone to more indurated siliceous claystone and porcellanite. The sediment chemistry (Murray et al., this volume), however, does not record the transition as precisely and subtly as the interstitial-water chemistry. Throughout the opal-CT–bearing intervals, dissolved silica concentrations decrease sequentially and finally reach minima at each site in the deepest interstitial-water sample, usually retrieved from beneath the higher temperature opal-CT/quartz diagenetic transition. There is no sharp decrease in dissolved silica associated with the opal-CT/quartz diagenetic transition, although this transition was not sampled in detail at any site.

The opal-A/opal-CT transition profoundly affects virtually all other interstitial-water chemical profiles because of the porosity and permeability decreases associated with the formation of opal-CT (Nobes et al., this volume, chapter 1). Thus, the opal-A/opal-CT diagenetic transformation effectively divides each site into two diffusive regimes, with the upper section reflecting strong communication with seawater and the section below the transition affected dominantly by basement alteration reactions. This effect is most clearly seen in profiles of the alkali elements involved in basement alteration reactions at depth (described in the following). For example, the decreasing K gradient at Sites 794, 795, and 797 averages 0.030 ± 0.007 mM/m above the opal-A/opal-CT transition, whereas below the transition the gradient shallows to 0.007 ± 0.003 mM/m.

CARBONATE CHEMISTRY

Variations in interstitial-water Ca, Mg, and Sr profiles have been used by many workers to infer several different low-temperature chemical processes. For example, a linear change in the Mg/Ca ratio with depth suggests conservative behavior of Mg and Ca with, as described later in this paper, alteration of basaltic basement as the dominant process supporting such linear interstitial-water gradients within the sediment column (McDuff, 1981; Gieskes, 1983). Conversely, increases in dissolved Ca and decreases in dissolved Mg, with a nonlinear change in the Mg/Ca relationship, imply the existence of diagenetic reactions within the sediment column (McDuff and Gieskes, 1976; Gieskes, 1983). Reactions occurring within the sediments that influence interstitial-water concentrations of Ca, Mg, Sr, and alkalinity include organic matter decomposition (increasing alkalinity to interstitial waters), biogenic carbonate dissolution (adding Ca, Sr, and increasing alkalinity), and inorganic calcite formation (removing Ca and decreasing alkalinity), as well as dolomitization (adding Ca and removing Mg; Sayles and Manheim, 1975; Baker, 1981; Gieskes, 1983; Gieskes et al., 1986). The alteration of volcanic ash, including the hydrolysis of volcanic glass and feldspar associated with clay-mineral formation, may also contribute Ca and Sr to interstitial waters (Lawrence et al., 1979; Gieskes et al., 1986). As many of these signals of interstitial-water processes are often similar, strict differentiation between the different fluid/solid reactions is not always possible.

At sites cored by Legs 127 and 128, the relative abundance of biogenic carbonate and the bulk-sediment accumulation rate determine which of the previously described processes exert the most significant influence on interstitial-water composition. As such, the respective carbonate processes influencing interstitial-water Ca, Sr, and alkalinity profiles can be considered as dominant at either the basinal or ridge sites.

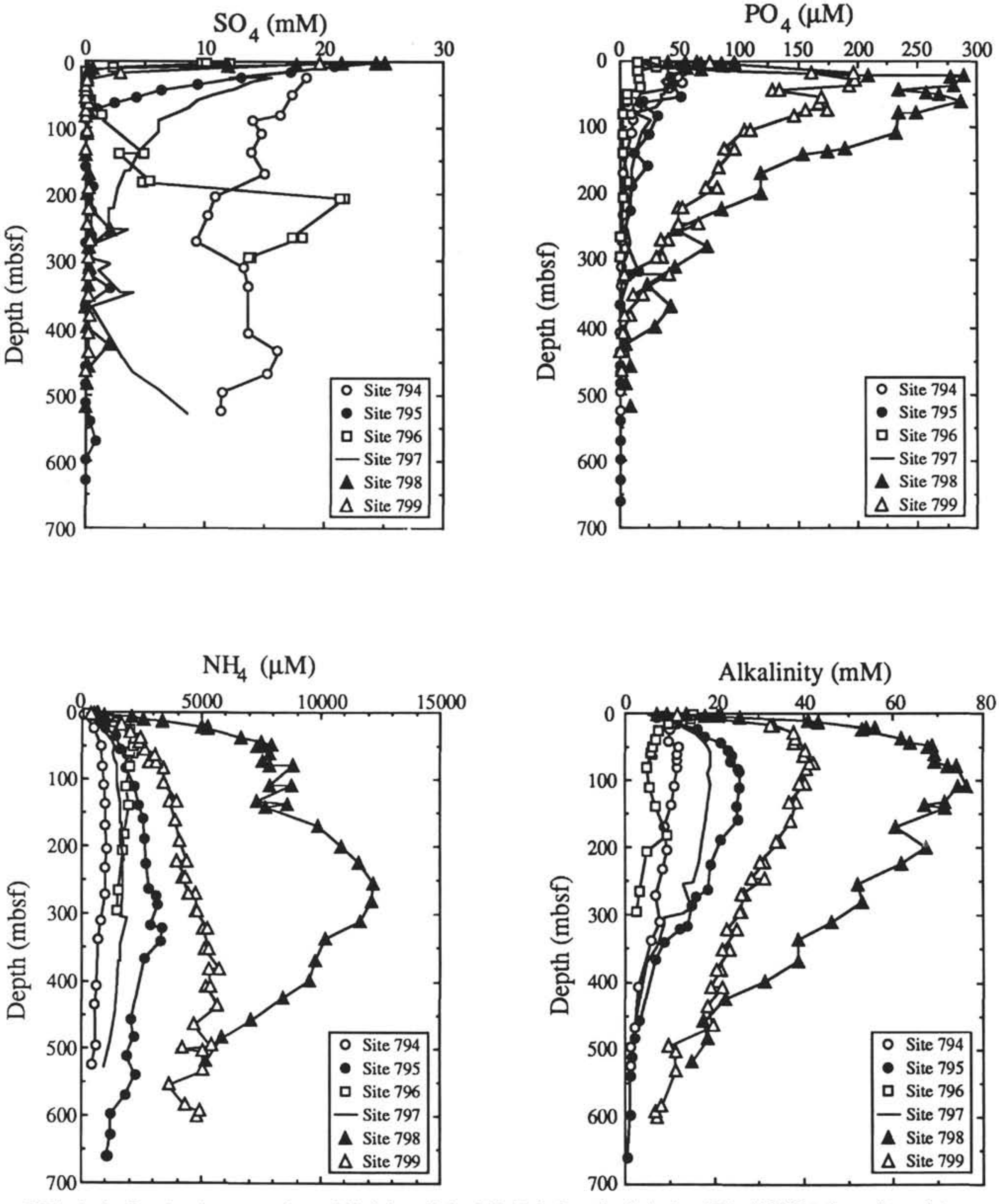

Figure 3. Dissolved sulfate, phosphate, ammonium, and alkalinity at all sites drilled in the Japan Sea during Legs 127 and 128. Note the consistency between all sites of the relative degree of sulfate utilization and generation of phosphate, ammonium, and alkalinity, with Sites 798 and 799 recording the earliest (i.e., shallowest) total depletion of sulfate and the greatest enrichment of organic metabolites. Site 794 records the least depletion of sulfate and smallest enrichment of metabolites. The sulfate increase with depth at Site 796 may reflect an original lack of metabolizable organic matter or replenishment of the sulfate reservoir by diffusion from seawater, aided by the relatively low sedimentation rate (Tamaki, Pisciotto, Allan, et al., 1990). Data from Tamaki, Pisciotto, Allan, et al. (1990) and Ingle, Suyehiro, von Breymann, et al. (1990).

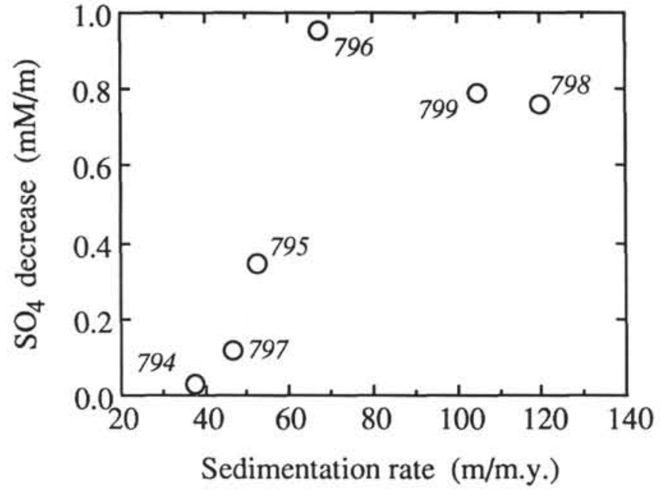

Figure 4. The empirical relationship recording the influence of the sedimentation rate on the preservation of organic matter (Berner, 1980), shown by plotting the dissolved interstitial-water sulfate gradient vs. bulk-sedimentation rate at all Leg 127 and Leg 128 sites.

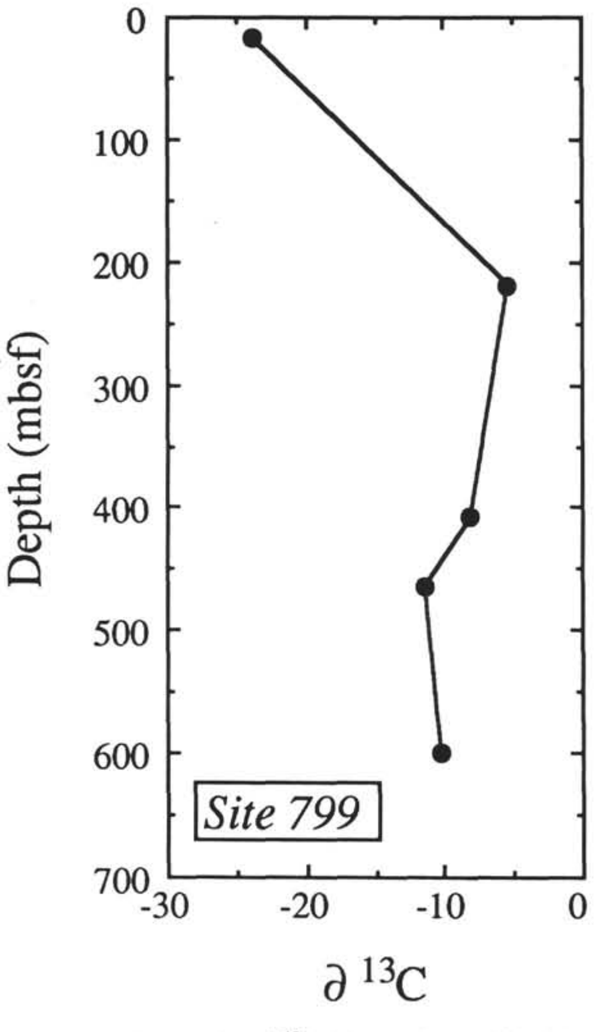

Figure 5. Depth distribution of $\delta^{13}C$ of the total dissolved CO_2 in the interstitial waters at Site 799, with the extreme depletion at 16 mbsf resulting from the oxidation of organic matter. Data from Sturz et al. (this volume).

At basinal sites (794, 795, and 797, with water depths exceeding 2800 m), sediments accumulate below the carbonate compensation depth (CCD) and at relatively low rates (5–77 m/m.y.; Tamaki, Pisciotto, Allan, et al., 1990). Calcareous biogenic components are absent or rare, and organic matter accumulation is slight. Interstitial-water alkalinity profiles are curved only slightly, when compared with alkalinity profiles at Sites 798 and 799 (Fig. 3). Dolomite is observed as hard layers, nodules, and crusts associated with units of relatively low permeability and high bulk density below the opal-A to opal-CT diagenetic transition (~300 mbsf). Profiles of dissolved Ca and Mg (Fig. 7A) are dominated by the strong influence of basement alteration, as described in detail later in this paper, although some changes in the interstitial-water Mg/Ca ratio (Fig. 7B) within the lithified units reflect dolomitization as well as basement alteration.

The water depth at the ridge sites (~1000 m for Sites 798 and 799) is shallower than at the basinal sites, and biogenic sediment components accumulating well above the CCD include calcareous nannofossils and foraminifers. Especially at Site 798, where sedimentation rates are high (average ~120 m/m.y.) and accumulating sediments are rich in organic carbon, alkalinity increases sharply below the sediment/water interface (Fig. 3). Calcium concentrations decrease (Fig. 7A), recording Ca removal into inorganic calcite, which is also independently suggested by the presence of carbonate rhombs as shallow as 25 mbsf. Mg/Ca profiles exhibit sharp maxima at 40 mbsf at Site 798 and 235 mbsf at Site 799 (Fig. 7B), reflecting the utilization of Mg and the release of Ca during dolomitization (Fig. 7A). These interstitial-water profiles are consistent with the presence of dolomite nodules and crusts below ~40 mbsf at Site 798 and below ~200 mbsf at Site 799.

Site 796 lies along the eastern flank of the Okushiri Ridge at a water depth of ~2600 m. The preservation of calcareous biogenic components at this site is poor, and sediment-accumulation rates range from 9 to 74 m/m.y. Interstitial-water alkaline earth metal profiles (Fig. 7A) at this site are difficult to interpret and reflect a combination of basement alteration, carbonate sediment diagenesis, and ash layer alteration. Dissolved Mg exhibits a minimum at ~50 mbsf, coinciding with the greatest frequency of ash layers. Dissolved Ca increases and dissolved Sr decreases within this same interval, suggesting that these two components are also influenced by ash alteration. Below the region of high ash accumulation (i.e., below ~100 mbsf), Ca and Mg trends are similar to those of the basin sites that reflect basement alteration and dolomitization.

BASEMENT ALTERATION

Processes of basement alteration are almost impossible to distinguish from the alteration of volcaniclastic materials (e.g., ash layers, "green tuff") within the sedimentary column or near the basement itself. The most sensitive indicators are stable and radiogenic isotopes, described in detail elsewhere (Brumsack et al., this volume). The major ions, and in particular the alkali and alkaline earth elements, also display concentration profiles notably indicative of basement alteration processes.

All sites drilled during Legs 127 and 128 are characterized by the depletion of Mg in interstitial fluids (Fig. 7A). Even though Mg removal may also be due to dolomite formation (see the preceding; Baker and Burns, 1985), alteration reactions involving smectites/illites and chlorites are most likely the major driving forces dictating the Mg/Ca decrease when approaching basement (Fig. 7B). These decreases are also accompanied by increases in Ca and Sr.

In addition to Mg removal, alkali metals are removed from interstitial waters at depth. Most notably, K decreases at all sites from near-seawater values at the sediment/water interface to near-zero values at basement (Fig. 8). Removal of K into altered basement rocks occurs in addition to the transformation of smectite to illite at the higher temperature regime within the lowermost sediment column. The K gradients at all Leg 127 and Leg 128 sites except Site 798 are essentially similar (Fig. 8). At Site 798, an increase in K is observed

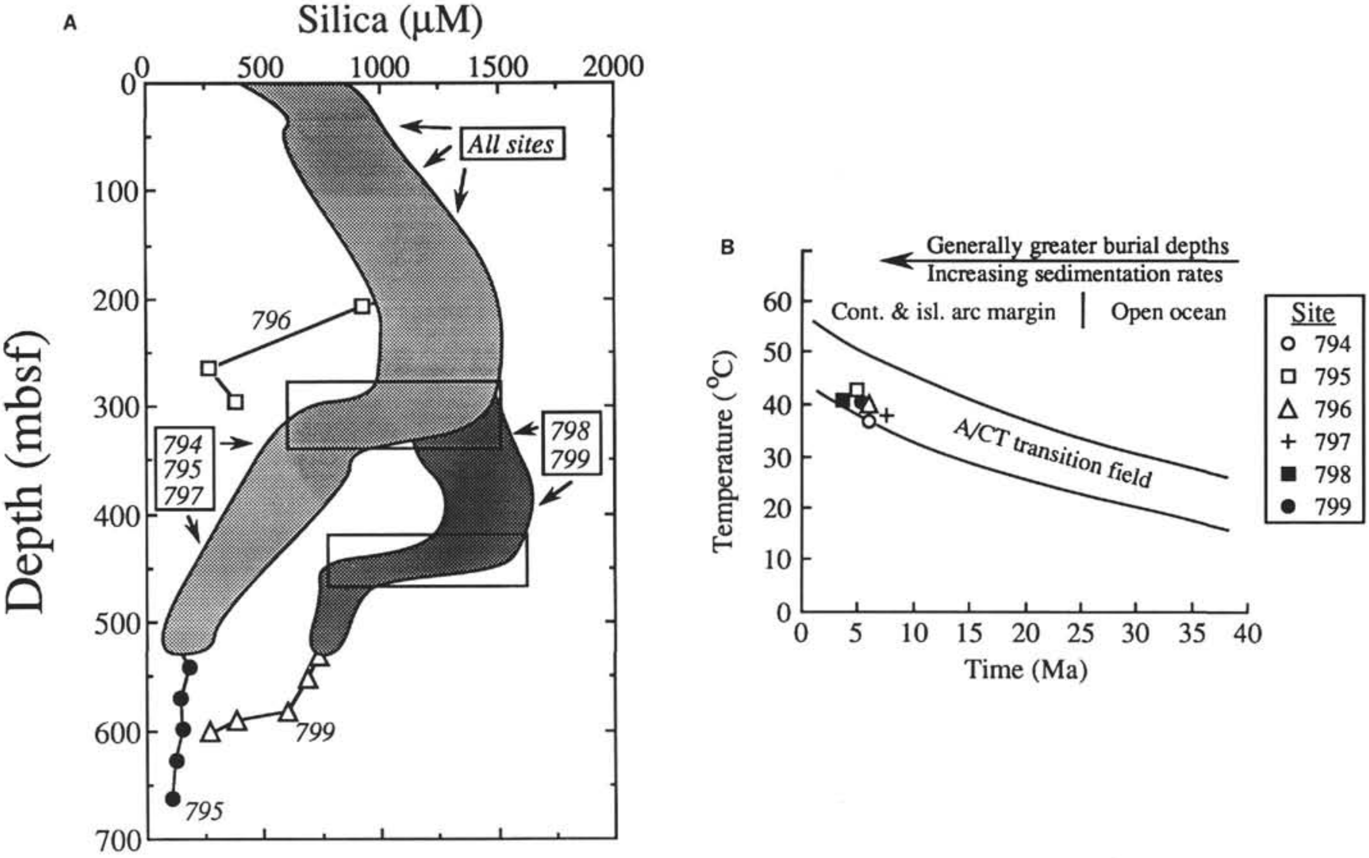

Figure 6. **A.** Synthesis of dissolved silica profiles at all Japan Sea ODP sites. Profiles overlay each other to ~300 mbsf, where the deep basinal Leg 127 sites experience the opal-A/opal-CT diagenetic transition (upper rectangle), resulting in a sharp decrease in dissolved silica. Sites 798 and 799 record the diagenetic transition at a greater depth (lower rectangle), due to the more gradual geothermal gradient. Note the consistency of behavior of dissolved silica in the deep basin sites vs. the relatively shallow Leg 128 sites. The profile at Site 796 reflects the varied sediment composition (e.g., common coarse sands), as well as the post-depositional tectonic uplift of the Okushiri Ridge. **B.** Time-temperature plot illustrating conditions for the initiation of opal-CT formation in moderately to highly siliceous marine sediment (from Hein et al., 1978). The opal-A/opal-CT transition at all Japan Sea ODP sites plots within this field and is consistent with the occurrence of opal-CT in other continental–island arc marginal basin environments.

from the sediment/water interface to ~400 mbsf, possibly related to the buildup of high NH_4 concentrations and resulting ion-exchange reactions with the solid phases (Gieskes et al., 1982). At greater depths, K is removed from the interstitial waters, as at the other sites. Note also that the ash alteration reactions at Site 796 (Tamaki, Pisciotto, Allan, et al., 1990) seem to have no influence on the interstitial-water K gradient.

Rb was analyzed only at the Leg 127 sites (794–797). In general, Rb concentrations decrease with depth (Fig. 9), with the lowest concentrations occurring near basement. In contrast to K, the Rb profiles show more scatter and suggest an involvement in ash alteration reactions within the sediment column. This is especially apparent at Site 796, where Rb concentrations are very low at ~50 mbsf, within the zone of abundant volcaniclastic material (Tamaki, Pisciotto, Allan, et al., 1990). Rb, like K, also is removed during deep basement alteration during the formation of authigenic clay minerals.

In contrast to the relatively straightforward behavior of K and Rb, Li exhibits more complicated profiles (Fig. 10). Li maxima seem to be associated with silica recrystallization reactions at the opal-A/opal-CT boundary. Below this zone, Li is removed from interstitial water and incorporated into alteration products of volcaniclastic material and basement rocks. This argument that Li is incorporated into basement alteration products is also supported by the empirical relation between $\delta^{18}O$ and Li found for altered spilitic rocks (Mengel and Hoefs, 1990). Similarly, the correlations between $\delta^{18}O$ and δD with K and Rb (Fig. 11) also suggest that basement alteration reactions are responsible for the overall observed depletions in alkali metal concentrations described earlier.

Site 795 records the strongest influence of basement alteration reactions on interstitial-water profiles in the Japan Sea. Na is considerably depleted only at this site (Fig. 12), with the substantial Na removal (~50% relative to seawater) reflecting albitization reactions at depth. Site 795 also exhibits the greatest decrease in $^{87}Sr/^{86}Sr$ (Brumsack et al., this volume) and is also the only site in the Japan Sea where Mg is totally depleted from interstitial waters (Fig. 7A).

In addition to the described alkali and alkaline earth elements, B is removed from interstitial fluids during low-temperature reactions with Japan Sea basement rocks, as suggested by the fact that the lowest B concentrations are observed at depth at all sites investigated (Brumsack et al., this volume). This is consistent with previous works that have shown that altered oceanic crustal rocks are commonly enriched in B (Spivack, 1986). Additionally, at Site 795 the $\delta^{11}B$ values of the interstitial waters are severely influenced by basement alteration processes, which drives the $\delta^{11}B$ of the interstitial waters toward values more than 20 ‰ lighter than seawater (Brumsack et al., this volume).

CONCLUSIONS

Diagenetic reactions within sediment columns throughout the Japan Sea record the influence of the bacterial degradation of organic matter, transformation of amorphous biogenic opaline silica to opal-CT, and formation and subsequent alteration of carbonate phases, as well as alteration of crystalline basement and volcanic ash. At each site, and through different stratigraphic intervals, the relative significance of these signals on the major, trace, and isotopic signatures recorded by the interstitial waters varies.

Organic matter oxidation significantly affects the chemistry of interstitial waters and sediments of the Japan Sea, not only with respect to the distribution of oxidants (SO_4, Mn, and CO_2) and dissolved metabolites (alkalinity, NH_4, and PO_4), but also in terms of the generation of authigenic solid phases. Site 794, located deep in the Yamato Basin, is the only site where sulfate is not completely consumed, whereas Sites 798 and 799 (both of which are ridge sites) record shallow total consumption of sulfate and concomitant extreme generation of alkalinity, NH_4, and PO_4. Formation of authigenic carbonates (Matsumoto, this volume), phosphate nodules (Föllmi and von Breymann, this volume), and barite (von Breymann et al., this volume) further highlight the importance of bacterial activity within the sediment column.

The opal-A/opal-CT diagenetic transition serves everywhere as a notable chemical, diagenetic, and stratigraphic horizon. This silica phase transition occurs more shallowly in the basinal sites (794, 795, and 797) because of the greater geothermal gradient found in the deep basin relative to the shallow ridge sites (798 and 799). Due to its effect on the porosity and permeability of the involved lithologies, the opal-A/opal-CT transformation effectively restricts many reactions in the uppermost interstitial-water column from those involved in the deep basement alteration. This phenomenon is most clearly seen in interstitial-water profiles of the alkali elements.

Processes that influence dissolved Ca, Mg, Sr, and alkalinity in interstitial waters from Japan Sea sediments are preferentially dominant at either the basin or ridge sites. At the basin sites, where sediment accumulation occurs relatively slowly and below the CCD, basement alteration is the dominant influence on dissolved Ca and Mg profiles. At ridge sites, where sediment accumulation is relatively fast and occurs above the CCD, diagenetic reactions within the sediment column, such as biogenic calcite dissolution, inorganic carbonate precipitation, dolomitization, and siderite/ankerite formation, are most significant.

Basement alteration reactions at depth and ash alteration within the sediment column together are responsible for downhole decreases in the interstitial-water concentrations of Mg, K, Rb, Li, B, $\delta^{18}O$, δD, $^{87}Sr/^{86}Sr$, and Na, as well as for increases in Ca and Sr. Again, many of these reactions are emphasized at depth not only because of the large degree of basement alteration, but also because of the isolating effect of the opal-A/opal-CT siliceous phase transition. Site 795, in the Japan Basin, records the greatest amount of basement alteration, as evidenced by the Na, $^{87}Sr/^{86}Sr$, and Mg profiles. Overall, the gradients resulting from basement alteration document the importance of the diffusive exchange of chemical constituents between endogenic and exogenic reservoirs. The chemistry of the altered basement rocks is influenced by reactions with the interstitial waters, whereas the newly formed clay minerals within the lower sediment column contain isotopic signals from the basement rocks.

ACKNOWLEDGMENTS

We thank K. C. Ruttenberg and Alan M. Shiller for their helpful comments and suggestions during review. We would like to further thank the extremely helpful technical staff of the ODP shipboard personnel on board both Leg 127 and Leg 128, particularly MaryAnn Cusimano, Luis Alvarez, Matt Mefferd, Barry Weber, Don Sims, Valerie Clark, Joe Powers, Wendy Autio, and William Mills. We also thank all the co-chief scientists (J. Ingle, K. Pisciotto, K. Suyehiro, and K. Tamaki) for their terrific support of the respective interstitial-water programs. H.-J. Brumsack acknowledges the scientific and analytical support provided by J. Hoefs, H. Nielsen, U. Haack, and R. Przybilla, as well as financial funding by the German ODP SPP (German Science Foundation). Research was funded by JOI/USSAC Cruise Science Support grants to R. W. Murray, A. A. Sturz, and M. T. von Breymann. This work was performed while R. W. Murray held a shore-based JOI/USSAC Ocean Drilling Program Fellowship.

REFERENCES

Baker, P., 1981. The diagenesis of marine carbonate sediments: experimental and natural observations [Ph.D. dissert.]. Univ. of California, San Diego.

Baker, P. A., and Burns, S. J., 1985. Occurrence and formation of dolomite in organic-rich continental margin sediments. *AAPG Bull.*, 69:1917–1930.

Balzer, W., 1984. Organic matter degradation and biogenic element cycling in a nearshore sediment (Kiel Bight). *Limnol. Oceanogr.*, 29:1231–1246.

Berner, R. A., 1980. *Early Diagenesis, A Theoretical Approach:* Princeton, NJ (Princeton Univ. Press).

Emerson, S., and Bender, M., 1981. Carbon fluxes at the sediment-water interface of the deep-sea: calcium carbonate preservation. *J. Mar. Res.*, 39:139–162.

Froelich, P., Klinkhammer, G., Bender, M., Luedtke, N., Heath, G. R., Cullen, D., Dauphin, P., Hammond, D., Hartman, B., and Maynard, W., 1979. Early oxidation of organic matter in pelagic sediments of eastern equatorial Atlantic: suboxic diagenesis. *Geochim. Cosmochim. Acta*, 43:1075–1090.

Gieskes, J. M., 1983. Interstitial waters of deep sea sediments. *In* Chester, J. P., and Riley, R. (Eds.), *Chemical Oceanography* (Vol. 6): New York (Academic Press), 221–269.

Gieskes, J. M., Elderfield, H., Lawrence, J. R., Johnson, J., Meyers, B., and Campbell, A., 1982. Geochemistry of interstitial waters and sediments, Leg 64, Gulf of California. *In* Curray, J. R., Moore, D. G., et al., *Init. Repts. DSDP*, 64 (Pt. 2): Washington (U.S. Govt. Printing Office), 675–694.

Gieskes, J. M., Elderfield, H., and Palmer, M. R., 1986. Strontium and its isotopic composition in interstitial waters of marine carbonate sediments. *Earth Planet. Sci. Lett.*, 77:229–235.

Hein, J. R., Scholl, D. W., Barron, J. A., Jones, M. G., and Miller, J., 1978. Diagenesis of late Cenozoic diatomaceous deposits and formation of the bottom simulating reflector in the southern Bering Sea. *Sedimentology*, 25:155–181.

Ingle, J. C., Jr., Suyehiro, K., von Breymann, M. T., et al., 1990. *Proc. ODP, Init. Repts.*, 128: College Station, TX (Ocean Drilling Program).

Lawrence, J. R., Drever, J. J., Anderson, T. F., and Bruekner, H. K., 1979. Importance of alteration of volcanic material in the sediments of Deep Sea Drilling Program Site 323. *Geochim. Cosmochim. Acta*, 43:573–588.

Manheim, F. T., and Sayles, F. L., 1974. Composition and origin of interstitial waters of marine sediments based on deep sea drill cores. *In* Goldberg, E. D. (Ed.), *The Sea* (Vol. 5): New York (Wiley-Interscience), 527–568.

McCorkle, D. C., 1987. Stable carbon isotopes in deep sea porewaters: modern geochemistry and paleoceanographic applications [Ph.D. dissert.]. Univ. Washington.

McDuff, R. E., 1981. Major cation gradient in DSDP interstitial waters: the role of diffusive exchange between seawater and the upper crust. *Geochim. Cosmochim. Acta*, 45:1705–1713.

McDuff, R. E., and Gieskes, J. M., 1976. Calcium and magnesium profiles in DSDP interstitial waters: diffusion or reaction? *Earth Planet. Sci. Lett.*, 33:1–10.

Mengel, K., and Hoefs, J., 1990. Li-$\delta^{18}O$ systematics in volcanic rocks and mafic lower crustal granulite xenoliths. Earth Planet. Sci. Lett., 101:42–53.

Rosenfeld, J. K., 1979. Ammonium adsorption in nearshore anoxic sediments. *Limnol. Oceanogr.*, 24:356–364.

Sayles, F. L., and Manheim, F. T., 1975. Interstitial solutions and diagenesis in deeply buried marine sediments: results from the DSDP. *Geochim. Cosmochim. Acta*, 39:103–127.

Spivack, A. J., 1986. Boron isotope geochemistry [Ph.D. dissert.]. Woods Hole Oceanographic Institute/MIT, Boston.

Tamaki, K., Pisciotto, K., Allan, J., et al., 1990. *Proc. ODP, Init. Repts.*, 127: College Station, TX (Ocean Drilling Program).

Wlotzka, F., 1972. Nitrogen. *In* Wedepohl, K. H. (Ed.), *Handbook of Geochemistry* (Vol. 2): Berlin (Springer Verlag), Sect. 7K.

Date of initial receipt: 11 July 1991
Date of acceptance: 13 November 1991
Ms 127/128B-177

A

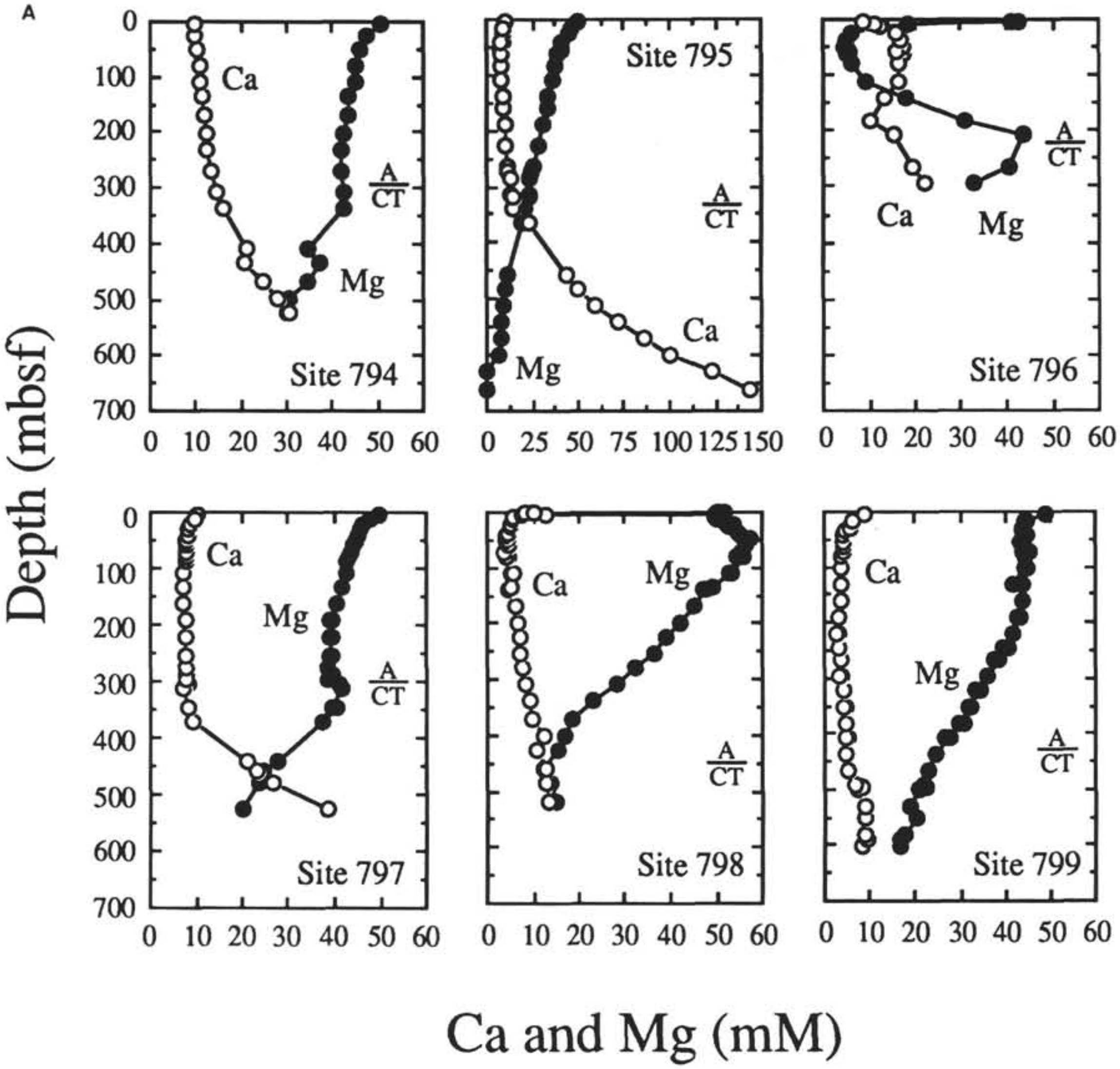

Figure 7. **A.** Downhole profiles of Ca and Mg at all Japan Sea ODP sites. Note the change in the horizontal scale for profiles at Site 795; the extreme Ca enrichment in the deeper pore fluids and the concomitant depletion of Mg reflect basement alteration reactions. A/CT indicates the position of the opal-A/opal-CT diagenetic phase transition. Data from Tamaki, Pisciotto, Allan, et al. (1990) and Ingle, Suyehiro, von Breymann, et al. (1990). **B.** Profiles of Mg/Ca at all Japan Sea ODP sites. See the text for discussion of the effects of dolomitization on the Mg/Ca ratio. A/CT indicates the position of the opal-A/opal-CT diagenetic phase transition.

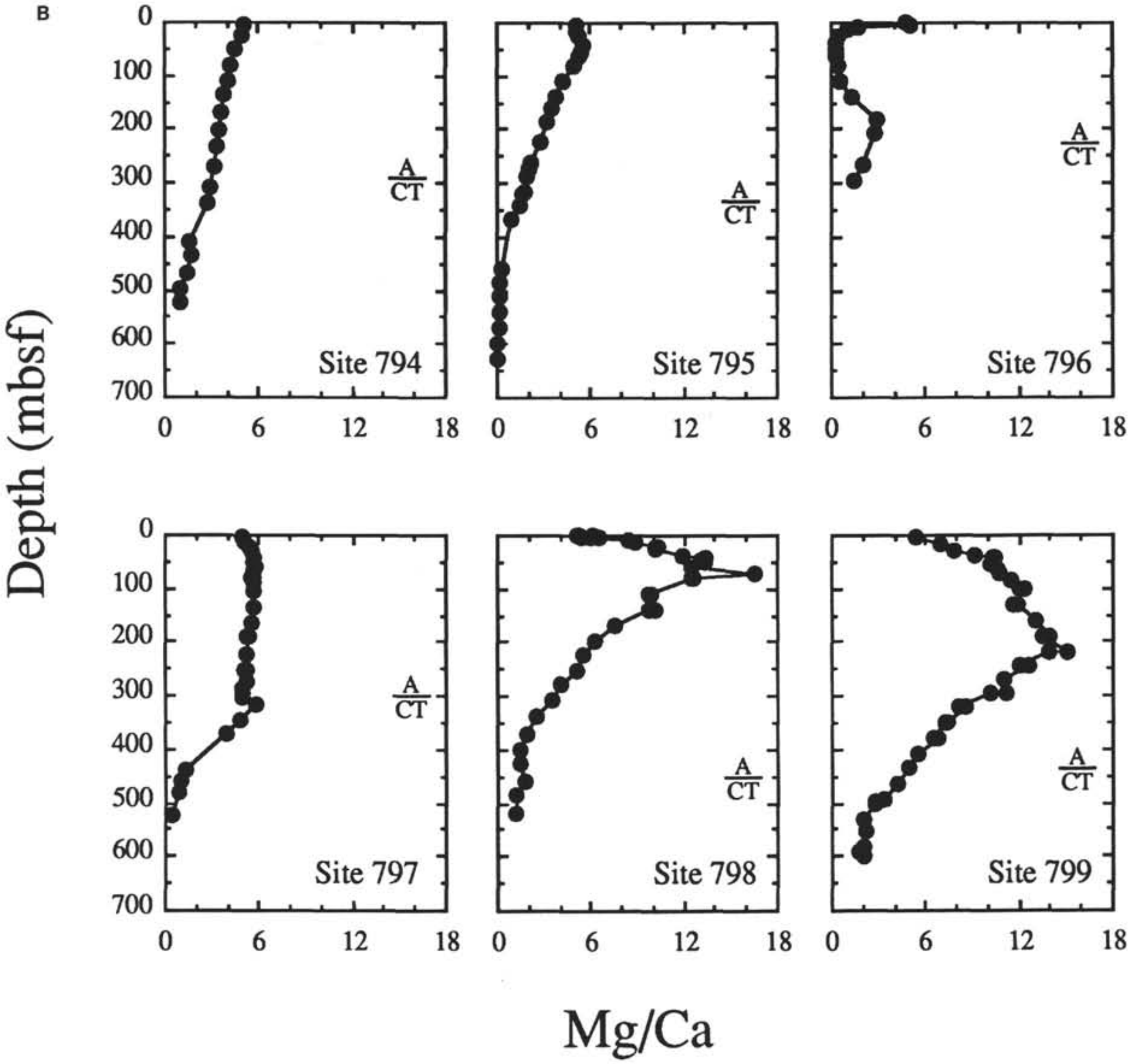

Figure 7 (continued).

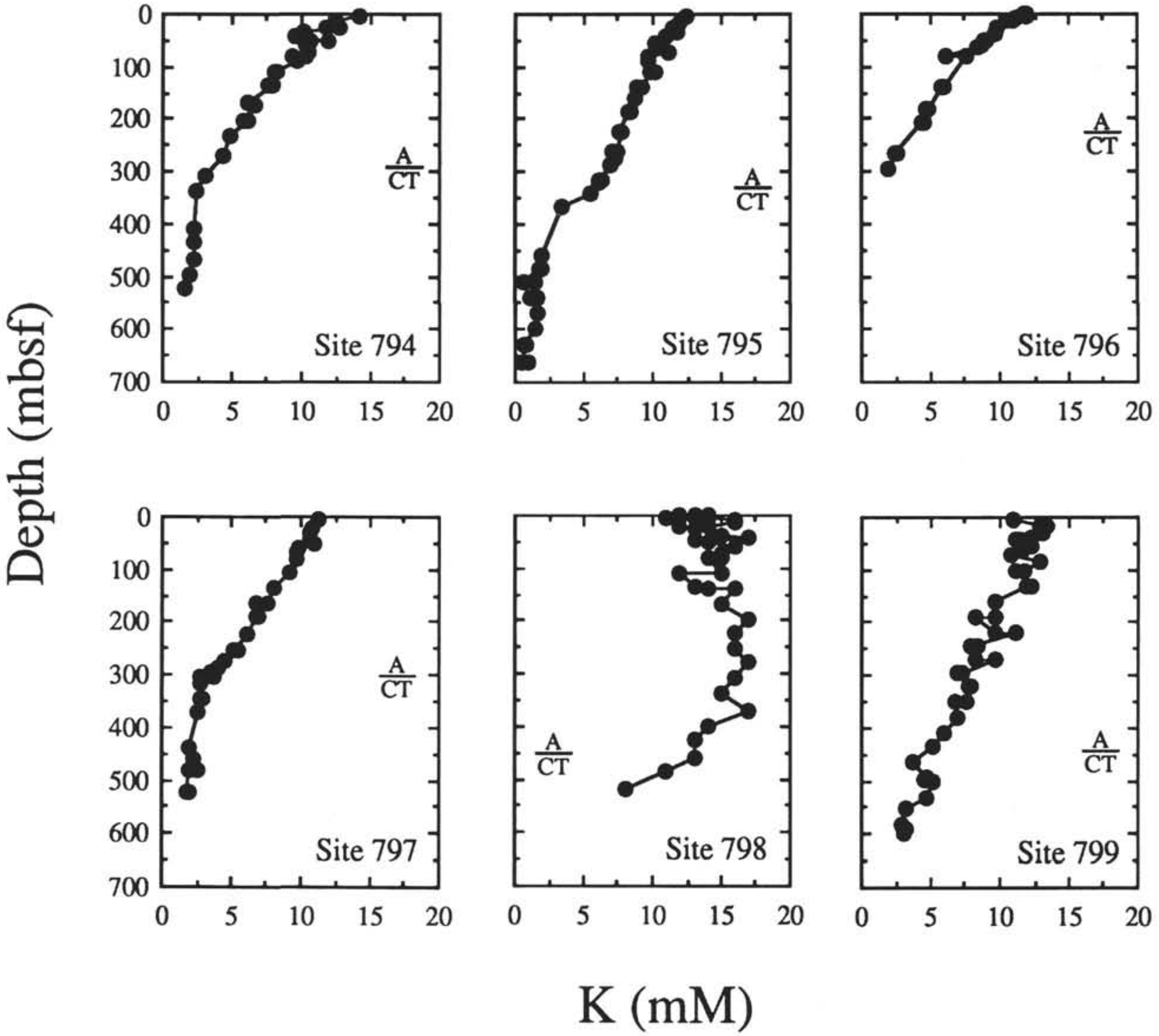

Figure 8. Profiles of K at all Japan Sea ODP sites, with the removal of K into altered basement rocks and the transformation of smectite to illite both resulting in the observed K depletion at depth. Note the clear demarcation of the opal-A/opal-CT transition (A/CT) at each site by the change in K gradient with depth.

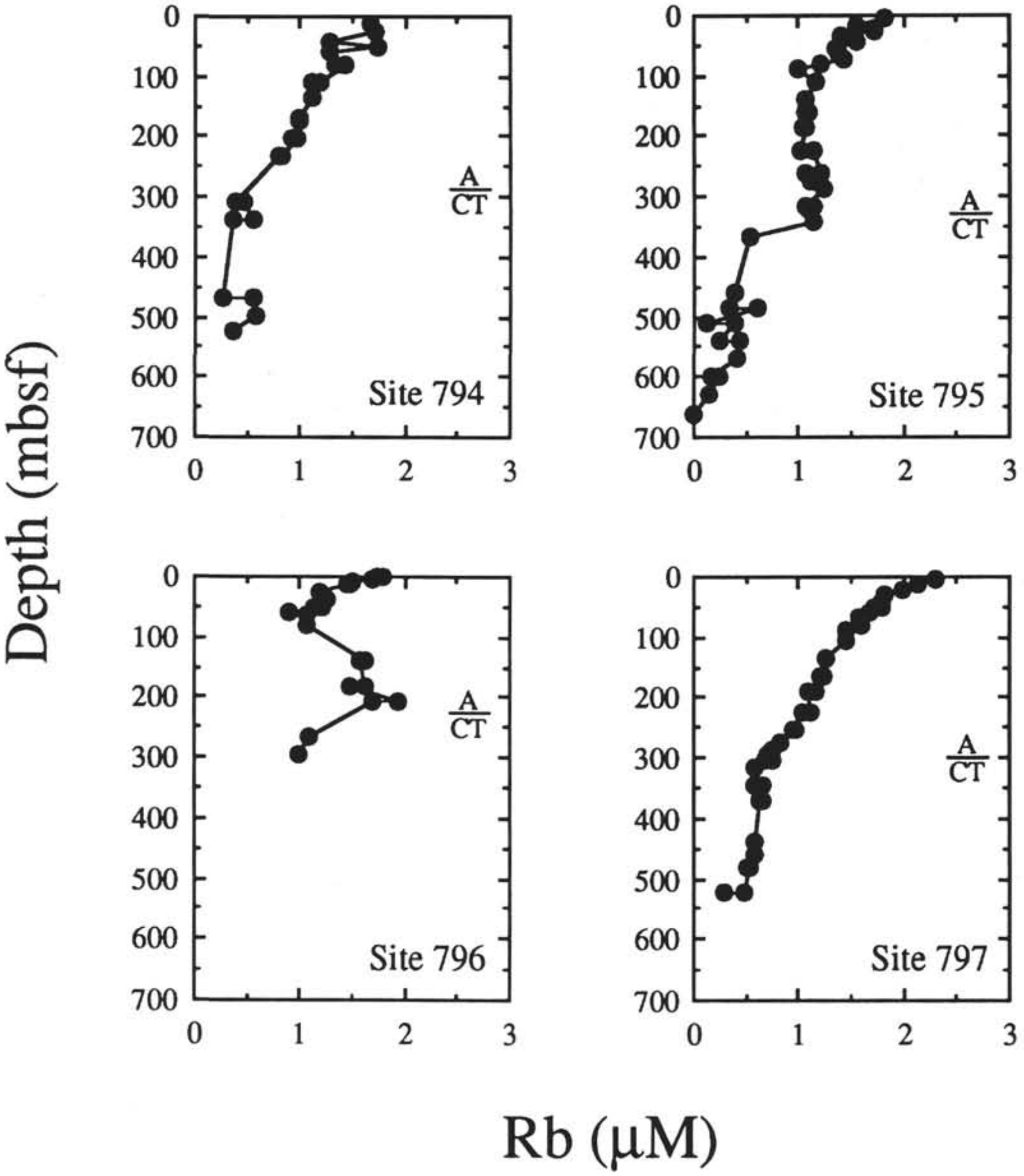

Figure 9. Profiles of Rb at all Japan Sea ODP sites. Although Rb is removed into basement alteration products along with K (Fig. 8), the greater amount of scatter higher in the sediment column, which is most visible at Site 796, suggests a further influence by the alteration of disseminated volcanic ash. A/CT indicates the position of the opal-A/opal-CT diagenetic phase transition.

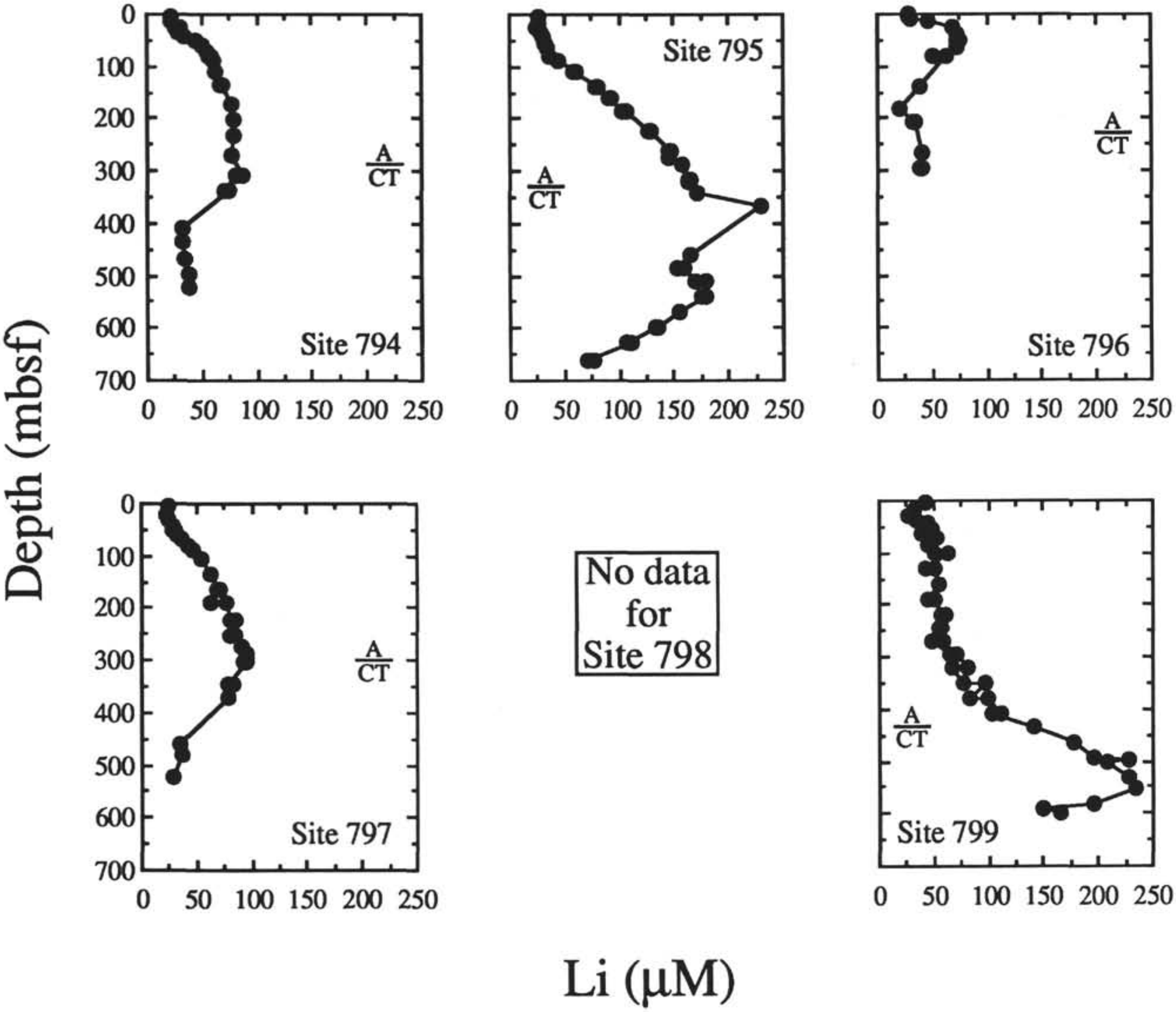

Figure 10. Profiles of Li at all Japan Sea ODP sites. In addition to suggesting a release by dissolving diatom tests (compare these Li profiles with the silica profiles shown in Fig. 6A), Li removal at depth is likely due to the formation of alteration products of volcanic ash and crystalline basement rocks. A/CT indicates the position of the opal-A/opal-CT diagenetic phase transition.

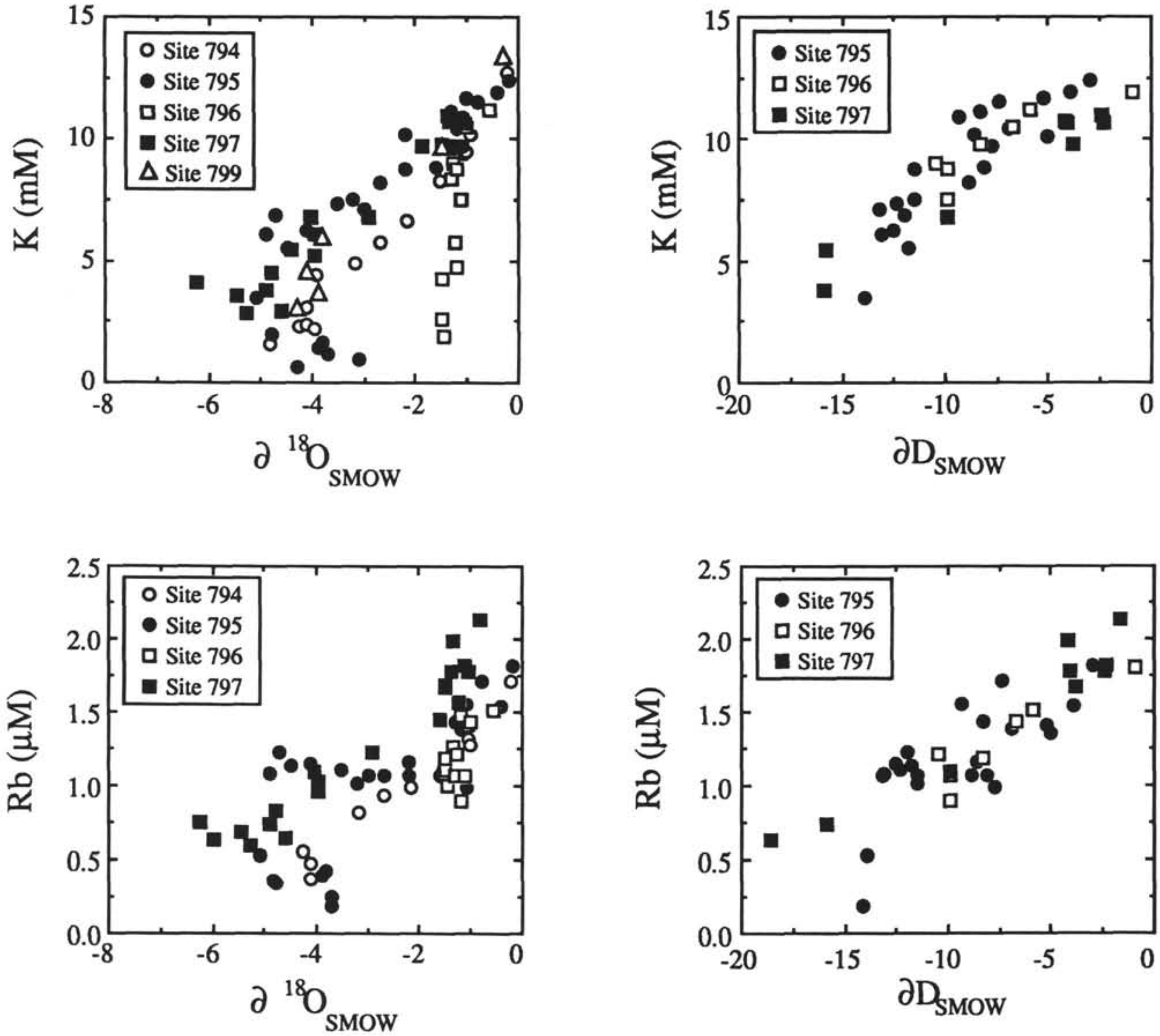

Figure 11. Well-defined positive correlations between $\delta^{18}O$ and δD with K and Rb confirm that the uptake of the alkalies by basement alteration reactions is responsible for the decreasing downhole K and Rb profiles of Figures 8 and 9.

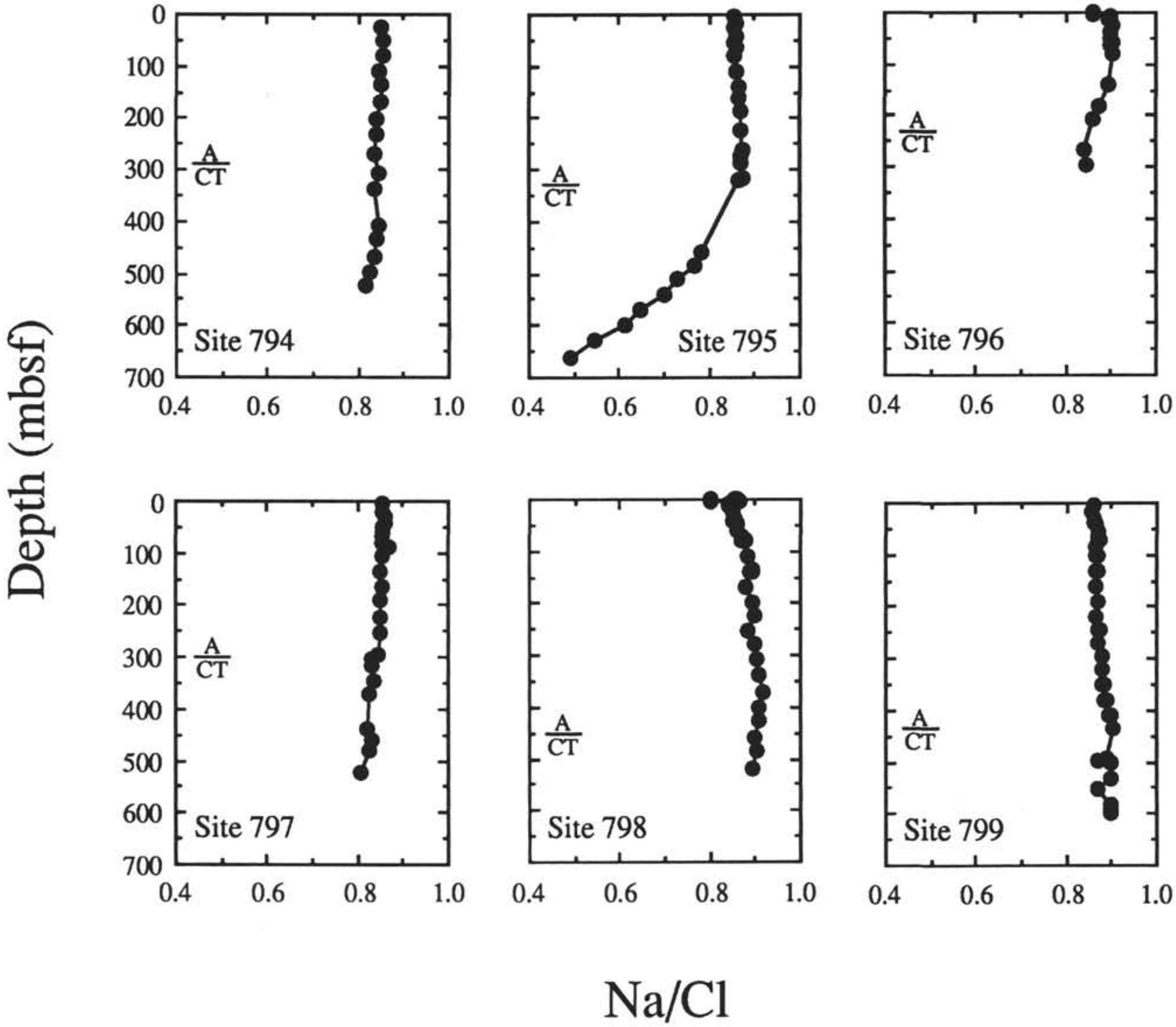

Figure 12. Profiles of Na/Cl (calculated by charge balance) at all Japan Sea ODP sites. The sharp decrease in Na/Cl at Site 795 below the opal-A/opal-CT transition reflects the large-scale removal of Na into albitization reactions at depth. No other site records such a strong influence of basement alteration; this site also records the greatest basement alteration effect on $^{87}Sr/^{86}Sr$ (Brumsack et al., this volume) and Mg (see text; Fig. 7A). A/CT indicates the position of the opal-A/opal-CT diagenetic phase transition.